Orientation and Protein−Cofactor Interactions of Monosubstituted *n*-Alkyl Naphthoquinones in the A_1 Binding Site of Photosystem I

Yulia N. Pushkar, Stephan G. Zech, and Dietmar Stehlik*

Institut für Experimentalphysik, Freie Universität Berlin, Arnimallee 14, D-14195 Berlin, Germany

Sarah Brown and Art van der Est*

Department of Chemistry, Brock University, 500 Glenridge Ave., St. Catharines, Ontario, L2S 3A1, Canada

Herbert Zimmermann

Max-Planck Institut für medizinische Forschung, Jahnstrasse 29, D-69120 Heidelberg, Germany

Received: July 20, 2002; In Final Form: September 20, 2002

1,4-Naphthoquinone (NQ) and its monosubstituted derivatives, 2-methyl, 2-ethyl, and 2-butyl-1,4-naphthoquinone, have been incorporated into the A_1 binding site of photosystem I (PS I) after organic solvent extraction of the native phylloquinone. The charge separated state $P_{700}^{+}NQ^{-}$ has been studied by multifrequency transient EPR. The Q-band (35 GHz) spectra of fully deuterated 2-methyl-1,4-NQ-d_8 and 2-ethyl-1,4-NQ-d_{10} show sufficient spectral resolution for the orientation of the quinone *g* tensor and thus the headgroup of the molecule to be determined. All orientation parameters of the substituted NQs are found to be the same as those established for native phylloquinone in PS I. However, for 2-ethyl-1,4-NQ and 2-butyl-1,4-NQ the X- and Q-band spectra exhibit a well resolved 1:2:1 hyperfine splitting. From the fact that it is absent when the first methylene group of the side chain is selectively deuterated, the splitting is assigned to the hyperfine coupling of the methylene protons. The principal values of the axially symmetric hyperfine coupling tensor are determined to be $|A_{xx}| = 12.2$ MHz, $|A_{yy}| = 16.8$ MHz, $|A_{zz}| = 12.2$ MHz, and $a_{iso} = 13.7$ MHz. The large methylene proton hyperfine coupling arises from a high spin density on the ring carbon atom to which the alkyl tail is attached. This in turn suggests that only one of the carbonyl groups of 2-alkyl-1,4-NQ is H-bonded to the protein and that the alkyl tail must be in the ortho position relative to the carbonyl group with the H bond. This implies that the alkyl side chain of the substituted NQs resides in the space normally occupied by the methyl group of phylloquinone and not that of the phytyl tail, which is meta to the H-bonded carbonyl group according to the X-ray structure. In addition, the hyperfine tensor indicates that the first two C−C bonds of the alkyl tail must be coplanar with the aromatic ring. However, the X-ray structure of PS I shows, for the native phylloquinone, that the phytyl tail is bent out of the quinone plane with the second C−C bond.

Introduction

In all photosynthetic organisms, the conversion of sunlight into chemical potential occurs in a membrane-bound complex referred to as a photosynthetic reaction center (RC). In oxygenic photosynthesis, two such complexes, photosystem I (PS I) and photosystem II (PS II), function in tandem and are also the most important representatives of type I and type II reaction centers. With the elucidation of the crystal structure at 2.5 Å resolution,[1] our knowledge of the structural details of PS I has increased dramatically. However, the functional significance of many structural features remains unclear. This is particularly evident when the cofactors and their binding sites are compared in the two types of RCs. Both types of reaction centers share a common structural motif of a protein heterodimer (or homodimer) and two branches of electron acceptors extending across the photosynthetic membrane from the primary electron donor P, which is a chlorophyll dimer. However, within this basic structure, the properties of all components show a great deal of variability, sometimes even within RCs of a single species. On the stromal side of the membrane, both RC types have a quinone acceptor usually of different molecular identity (phylloquinone, plastoquinone, ubiquinone, etc.). However, in general, the same quinone can function in either type of RC. In type II RCs, there are two active quinones, one of which diffuses in and out of the reaction center carrying electrons and protons across the membrane, whereas in type I RCs, the quinones are not labile as part of their normal function, and the extent to which they are active in electron transfer has not yet been established unambiguously. EPR studies of PS I and RCs of purple bacteria[2−5] have shown that the orientation and electronic environment of the quinones in these two reaction centers differ greatly. The recently published 2.5 Å resolution X-ray structure of PS I has confirmed the difference in orientation of phylloquinone (PhQ) in the type I photosystem I RC versus ubiquinone in the type II RC of purple bacteria (pbRC).[1,6] Both quinones have a methyl group and an unsaturated hydrophobic tail as ring substituents at adjacent positions between the two C═O groups. However, the interactions between quinone and protein,

* To whom correspondence should be addressed. Dietmar Stehlik: Phone: 0049(30)83855069. Fax: 0049(30)83856081. E-mail: Stehlik@physik.fu-berlin.de. Art van der Est: Phone: +001-905-688-5550 ext. 4602. Fax: +001-905-682-9020. E-mail: avde@brocku.ca.

10.1021/jp0265743 CCC: $22.00
Published on Web 10/24/2002

such as hydrogen bonding and π stacking, are different. Questions related to how the protein−cofactor interactions control the quite different functional properties of the quinones in the two types of RC are largely unanswered. For instance, it is known that the redox potentials, H-bonding, electron transfer kinetics, and magnetic tensor properties of the quinones in the two RCs differ greatly, but it is not yet clear whether there is a correlated interplay between these various properties. Previous work with phylloquinone biosynthetic pathway mutants, in which the synthesis of phylloquinone was blocked, showed that plastoquinone (PQ-9 of PS II) can also function in PS I.[7] The orientation of the plastoquinone headgroup and the influence of H-bonding on the spin density were found to be the same as for phylloquinone. However, forward electron transfer from plastoquinone to F_X was slowed by an order of magnitude as a result of the slightly different redox potentials of plastoquinone and phylloquinone.[8] The role of the methyl group attached to the headgroup of phylloquinone was investigated by deleting the *men*G gene, which codes for the methyl transferase responsible for attaching the methyl group during the final step in the phylloquinone biosynthesis.[9] In the absence of the methyl transferase, 2-phytyl-naphthoquinone (i.e., phylloquinone without the methyl group) is incorporated into PS I. Again, no difference in the orientation and binding of the quinone was observed, and only a marginal slowing the forward electron transfer due to the change in redox potential was found. These results suggest that the methyl group does not play a critical role in determining the orientation of the quinone headgroup and it does not influence the function strongly.[9] On the other hand, one would expect that the phytyl side chain plays a more important structural role. All of the membrane bound cofactors in PS I have such a chain, and it is generally assumed that it is present to increase their hydrophobicity thus increasing their affinity for the membrane. It also seems likely that the side chain acts as an anchor holding the cofactors in place. However, this has not yet been tested.

Here, we report results for a series of naphthoquinone (NQ) derivatives incorporated into PS I particles after extraction of the native phylloquinone using organic solvents. The NQs have a single asymmetric ring substituent of *n*-alkyl character [$-(CH_2)_{(n-1)}-CH_3$]. The primary goal is to identify individually the specific roles of the phytyl tail and of the $-CH_3$ group in determining the orientation of the quinone headgroup and its binding to the protein. We will show that even a single methyl group, i.e., 2-methyl-1,4-NQ (VK_3), ensures the same orientation of the NQ headgroup as that of native phylloquinone. An unexpected result is that the NQs with a saturated alkyl chain as a single substituent bind in the A_1 site such that the alkyl chain assumes the position normally occupied by the phylloquinone methyl group and not that of the phytyl chain. This implies that just one asymmetric substituent is sufficient for proper orientation and thus even a single methyl substituent does in fact play an essential role in determining the orientation of the headgroup in the A_1 site.

Materials and Methods

Quinones. Various quinones and the reagents for the preparation of buffers were purchased from Aldrich. 2-Ethyl-1,4-naphthoquinone-d_{10} was prepared by oxidation of 2-ethylnaphthalene-d_{12} with CrO_3 in acetic acid. The perdeuteration of 2-ethylnaphthalene was accomplished by catalytic exchange with D_2O in a high-pressure vessel (6 days at 280 °C) with platinum on carbon as the catalyst. Three subsequent exchange reactions resulted in 2-ethylnaphthalene-d_{12} with $D = 98\%$ as confirmed by NMR and mass spectroscopy. 2-Ethyl-α,α-d_2-1,4-naphthalene was obtained by reduction of 2-methylnaphthyl ketone with $AlCl_3/LiAlD_4$ 1:1 under reflux in ether. The isolated and distilled product was oxidized to 2-ethyl-α,α-d_2-1,4-naphthoquinone with Cr(VI) oxide as described above. $D = 98\%$

Preparation of Photosystem I Samples. PS I isolated from *Synechocystis* PCC 6803 was prepared by the method of Biggins and Mathis.[10] The isolated PS I was lyophilized, and the native phylloquinone was removed by solvent extraction as described in refs 10 and 11 using hexane (99%, Aldrich) containing 0.3% methanol (Caledon). The extraction of the phylloquinone was monitored using a modified Bruker ESP 200 X-band spectrometer (described below) by measuring the disappearance of the spin polarized EPR signal due to $P_{700}{}^+A_1{}^-$ and accompanying appearance of $^3P_{700}$ formed by recombination from $P_{700}{}^+A_0{}^-$. The loss of other pigments was monitored using the visible absorption spectrum of the supernatant recorded with a Unicam UV−vis spectrometer. Samples for EPR analysis were prepared by suspending 15 mg of extracted PS I in 150 μL of buffer containing 50 mM Tricine, 10% glycerol, and 0.2% Triton X−100. A homogenizer was used to ensure complete resuspension. A series of quinones were introduced into the A_1 binding site by incubating the extracted PS I with an excess of quinone. The quinone (∼150 mM) was prepared in either ethanol, 1-propanol, or dimethyl sulfoxide solution and added to the resuspended PS I sample to give a 1000:1 molar ratio of quinone to PS I. The samples were then incubated in the dark at 4 °C, with incubation times ranging from 30 min to 3 h. The incorporation of quinone into the A_1 site was monitored by observing the appearance of a spin polarized EPR spectrum due to $P_{700}{}^+NQ^-$ accompanied by the disappearance of the $^3P_{700}$ spectrum. Control experiments using blanks of the three solvents containing no quinone were also performed and no change in the transient EPR spectra was observed. For the EPR experiments, 1 mM sodium ascorbate and 50 μM phenazine methosulfate were added as external redox agents, and the samples were frozen in the dark.

Transient EPR Spectroscopy. Control experiments and monitoring of the extraction and reconstitution of the quinone were carried out at X-band using a modified Bruker ESP 200 spectrometer equipped with a home-built, broad-band amplifier (bandwidth >500 MHz). A rectangular resonator and a liquid-nitrogen temperature control unit were used, and the samples were illuminated using a Q-switched, frequency doubled Continuum Surelite Nd:YAG laser at 532 nm with a repetition rate of 10 Hz.

All other X-band transient EPR experiments were carried out using a Bruker ER046 XK-T microwave bridge equipped with a Flexline dielectric resonator[12] and an Oxford liquid helium gas-flow cryostat. The loaded Q value for this dielectric ring resonator was about $Q = 3000$, equivalent to a rise time of $\tau_r = Q/(2\pi\nu_{mw}) \approx 50$ ns. Q-band (35 GHz) transient EPR spectra of the samples were also measured with the same setup except that a Bruker ER 056 QMV microwave bridge equipped with a home-built cylindrical resonator was used. The samples were illuminated using a Spectra Physics Nd:YAG/MOPO laser system operating at 10 Hz at either the 2nd harmonic 532 nm or near the long wavelength absorption edge of PS I at approximately 700 nm.

Results and Discussion

General Strategy. The molecular structures of the series of 1,4-naphthoquinone (NQ) derivatives introduced into the A_1 site of PS I are shown in Figure 1. These quinones, which have a

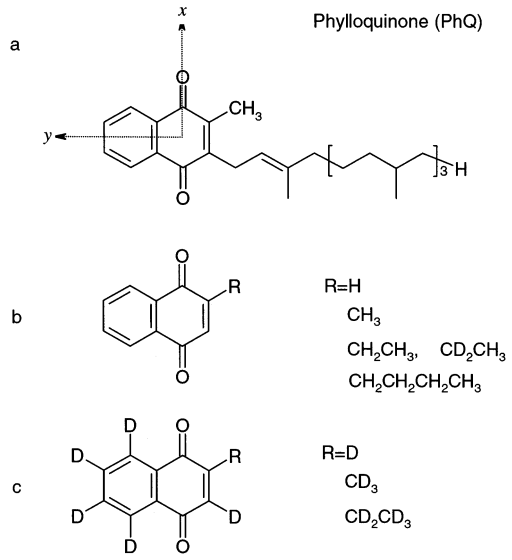

Figure 1. Molecular structure of naphthoquinone derivatives used. (a) Molecular structure of phylloquinone (PhQ; vitamin K_1), 2-methyl-3-phytyl-1,4-naphthoquinone) and *g*-tensor principal axes coinciding with the long and short inplane axes of the quinone ring. Note that the principal axes of the hfs tensors of the protons in the substituents deviate from the molecular *x*, *y*, and *z* axes, e.g., A_{II} for the nearly axially symmetric CH_3 hfs tensor is roughly parallel to the $C-CH_3$ bond. (b) Molecular structures of the protonated and partially deuterated 1,4-naphthoquinone derivatives used for incorporation into the A_1 site in PS I. (c) Molecular structures of the corresponding fully deuterated 1,4-naphthoquinone derivatives.

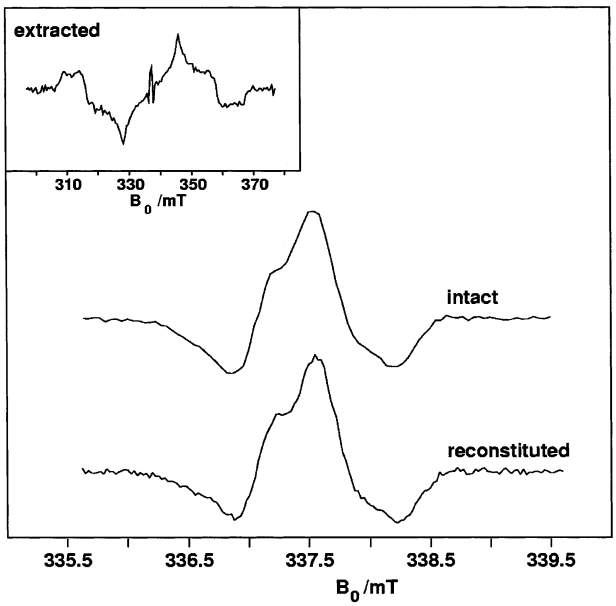

Figure 2. Spin polarized transient EPR spectra of $P_{700}^+A_1^-$ in PS I taken at X-band and 135 K before extraction (intact) and after extraction (extracted) and after reconstitution with PhQ (reconstituted). The inset shows the broad $^3P_{700}$ triplet spectra observed after extraction of the quinone. The small peaks at the center of the triplet spectrum are due to the small remaining fraction of reaction centers in which PhQ has not been removed. Note that the field axis covers a much wider range in the inset than in the main part of the figure.

single substituent at position 2 of the NQ ring, are intended to probe the role of the methyl group and phytyl tail in the protein−cofactor interactions of phylloquinone in the A_1 site. From the X-ray structure of PS I[1,6] and the magnetic properties of A_1^-,[13] it is known that phylloquinone is asymmetrically H-bonded to the protein via the C═O oxygen, ortho to the phytyl tail, and meta to the methyl group. In addition, a π-stacking arrangement exists between phylloquinone and a nearby tryptophan ($W697_{PsaA}$ or $W677_{PsaB}$). However, it is not known how the methyl and phytyl substituents influence these features individually. One series, 1,4-naphthoquinone, 2-methyl-1,4-naphthoquinone (vitamin K_3), and 2-phytyl-3-methyl-1,4-naphthoquinone (PhQ), is useful to test the necessity of both methyl group and phytyl tail or only the methyl group for fixing the proper orientation and function of the quinone in the A_1 site. Another series of quinones with a single saturated alkyl chain $[-(CH_2)_{(n-1)}-CH_3]$ of variable length (Figure 1b) is intended to replace the native phytyl tail with an alternative simpler chain. For example, with 2-methyl-1,4-naphthoquinone (VK_3) (i.e., $n = 1$), it is expected that the quinone will be incorporated with the methyl group in the same position as the methyl group in PhQ, i.e., meta to the H-bonded oxygen. On the other hand, for larger values of *n*, it is expected for simple space filling reasons that the alkyl group will assume the role of the phytyl tail in PhQ and resides ortho to the H-bonded oxygen. The hyperfine couplings of the alkyl substituents serve as an ideal observable for determining the location of the substituents relative to the H-bonded oxygen because they are conveniently measured and reflect the asymmetry in the spin density distribution induced by the asymmetric H bonding. The correct assignment of the hyperfine coupling to methyl and/or methylene protons can be assured unambiguously by selective deuteration. Finally, full deuteration of the 1,4-naphthoquinone derivatives (Figure 1c) is employed in order to reduce the inhomogeneous line width contribution due to unresolved hyperfine splittings and thus increase the *g*-tensor resolution and hence the accuracy in determining the orientation. Transient spin polarized EPR spectra of the functional radical pair state $P_{700}^+NQ^-$ contain information about the relative orientation of the cofactors involved, as well as about specific interactions with the protein environment via the hyperfine and *g*-tensor parameters.[5] Thus, they provide a convenient way of investigating the influence of NQ substituents on these binding properties.

Test of Functionality of PS I Particles after A_1 Extraction/Substitution. By definition, the procedure used to remove PhQ denatures the A_1 binding site. Therefore, it is important to ensure that this process is reversible and that no permanent damage or protein conformation changes occur. Figure 2 shows the result of a control experiment in which the extracted PS I has been reconstituted with PhQ. In the main part of Figure 2, the spin polarized transient EPR spectra of $P_{700}^+A_1^-$ are compared for intact PS I (top) and extracted PS I reconstituted with PhQ (bottom). As an insert, the spectrum of extracted PS I before reconstitution is shown on a wider field scale. The broad spectrum in the inset is due to the characteristic polarization pattern of the $^3P_{700}$ state formed by $P_{700}^+A_0^-$ recombination in reaction centers devoid of PhQ. The weak narrow peaks at the center of the inset spectrum are due to a minor fraction of reaction centers in which PhQ has not been removed. Clearly, incubation with PhQ (bottom spectrum) restores electron transfer to the quinone as indicated in the resulting $P_{700}^+A_1^-$ spectrum. The electron-transfer kinetics (not shown) are identical to those of intact PS I. Thus, we can conclude that the solvent extraction does not cause any permanent changes to the protein in the vicinity of the electron-transfer chain from P_{700} to A_1, despite the fact that it is known to remove a considerable fraction of the antenna chlorophylls and carotenoids. We cannot exclude that a small portion of the reaction centers is rendered inactive as a result of the quinone extraction/reconstitution procedure. An estimate from a comparison of the signal-to-noise ratios in Figure 2 is inappropriate because identical instrumental condi-

tions cannot be guaranteed in this case. However, following phylloquinone reconstitution, any remaining transient $^3P_{700}$ contribution is below detection limit (<10%).

PS I Containing 2-Alkyl NQ Derivatives. Figure 3 presents the X-band and Q-band spectra of the radical pair state $P_{700}^+NQ^-$ in a series of PS I samples containing 2-methyl-, 2-ethyl-, and 2-butyl-1,4-naphthoquinone. The transient EPR spectra of the three samples exhibit the same overall polarization pattern as native PS I, i.e., E/A/E (E = emission, A = absorption) at X-band and E/A/A/E/A at Q-band (Figure 3). Although the overall polarization does not change, the non-native quinones do have a dramatic effect on the partially resolved proton hyperfine structure (hfs). For native PS I, the methyl group in the meta position to the H-bonded oxygen leads to a resolved quartet with relative intensities 1:3:3:1 centered near the g_{yy} component of the quinone g tensor as result of a nearly axially symmetric hfs tensor with principal values (A_{xx} = 9.2 MHz, A_{yy} = 12.8 MHz, A_{zz} = 9.0 MHz).[14] The same hfs pattern is even more clearly resolved in the spectra from the samples incubated with 2-methyl-1,4-NQ (VK_3; Figure 3, second spectrum from top). This is readily explained if the spin density distribution over the NQ rings remains the same as for PhQ but the inhomogeneous line width is reduced because of the smaller number of unresolved proton hyperfine couplings when the nearby phytyl tail is absent. In native PS I, the partially resolved methyl hyperfine splitting is unusually large because the oxygen meta to the methyl group is involved in H-bonding, whereas the oxygen ortho to it is not.[1,13] This results in an alternating spin density distribution such that the spin density is increased on the ring carbon to which the methyl group is bound.[13−15] Thus, the spin polarization and hyperfine pattern observed with 2-methyl-1,4-NQ in the A_1 binding site suggest that it binds to the protein with the methyl group in the same position as for native PhQ.

In contrast, the well resolved hfs triplet with relative intensities 1:2:1 observed for the samples incubated with 2-ethyl- and 2-butyl-1,4-NQ (bottom spectra in Figure 3) has no correspondence in native PS I. The splitting pattern is due to two nearly equivalent protons and is assigned to the first methylene group of the alkyl chain. To verify this assignment independently, selective deuteration of the methylene group of 2-ethyl-1,4-NQ was used. As demonstrated in Figure 4, the 1:2:1 hyperfine pattern disappears if the methylene group of 2-ethyl-1,4-NQ is selectively deuterated (bottom spectrum in Figure 4). The splitting of the partially resolved hyperfine pattern gives an effective hfs constant for the methylene protons. A rough estimate from a qualitative inspection of spectra in Figures 3 and 4 yields a value of 16−17 MHz which is considerably larger than that of the methyl protons of 2-methyl-1,4-NQ. Thus, the spin density on the ring carbon adjacent to the alkyl group must be high. Consequently, the distortion of the spin density due to asymmetric H bonding is such that the alkyl group has to be meta to the oxygen with the H bond. If the 2-alkyl-1,4-NQ is also bound to the protein via a single H bond to Leu A722 (B706), this places the alkyl side chain in a position analogous to the methyl group in phylloquinone. This is a surprising result because one would expect that with increasing chain length steric hindrance would force the alkyl chain to reside in the space normally occupied by the phytyl tail of PhQ. Indeed, we have recently shown[9] that this occurs when 2-phytyl-1,4-NQ is incorporated into PS I by inhibiting the final methylation step in the biosynthesis of PhQ. In this case, a strong hfs is observed from the ring proton in the position occupied by the methyl group in PhQ, whereas the hfs from the methylene protons of the phytyl tail is too small to be resolved. Thus, as for PhQ, the ring carbon to which the phytyl tail is attached carries a

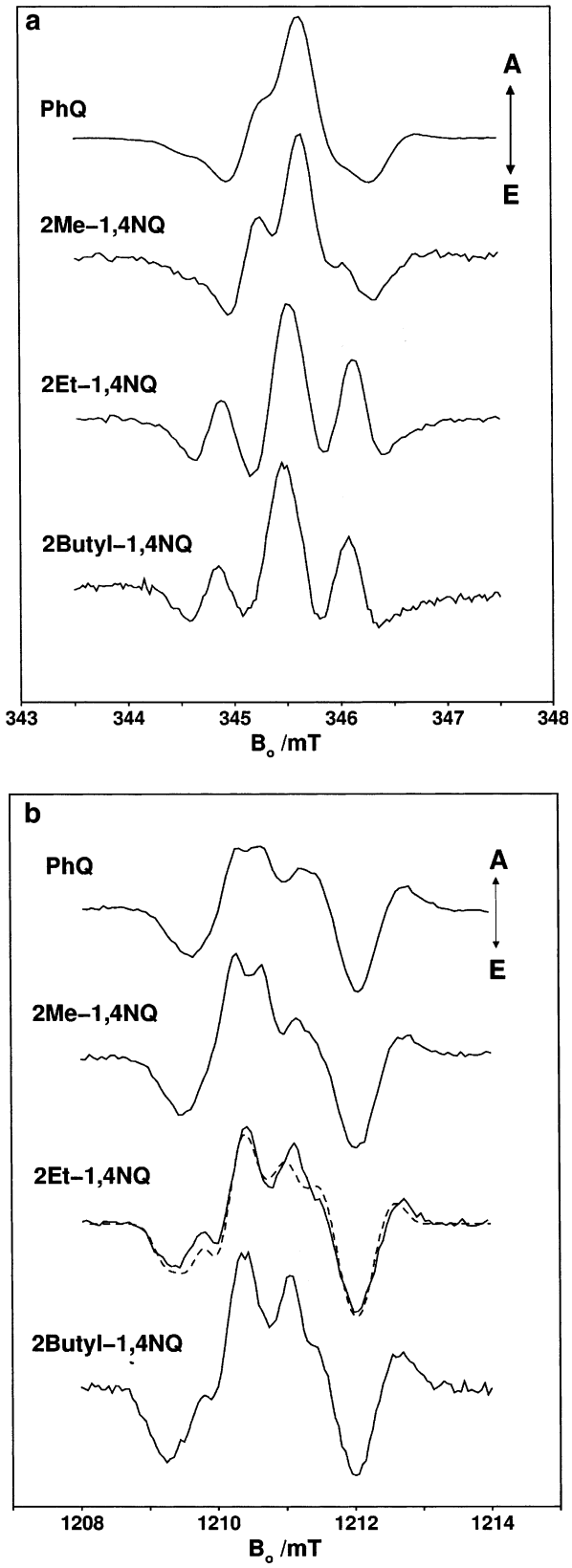

Figure 3. (a) X-band, 80 K spin polarized transient EPR spectra of $P_{700}^+NQ^-$ radical pair in PS I containing native phylloquinone (PhQ), 2-methyl-, 2-ethyl-, and 2-butyl-1,4-naphthoquinone in the A_1 binding site. (b) Corresponding Q-band, 80 K spin polarized transient EPR spectra of the same samples. The broken line curve is a simulated spectrum, calculated using the parameters given in Table 1.

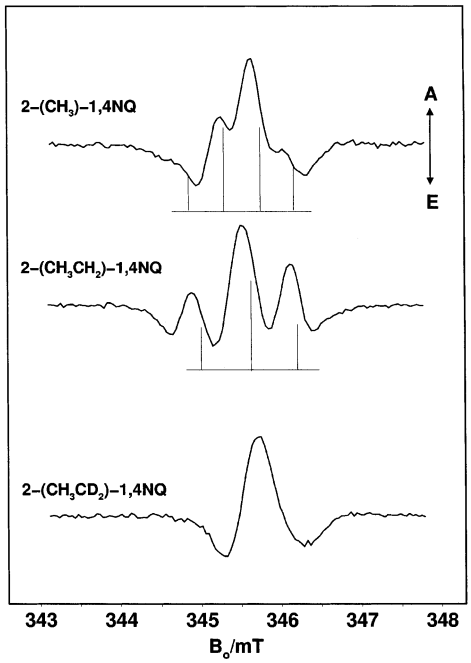

Figure 4. X band, 80 K spin polarized transient EPR spectra of $P_{700}^{+}NQ^{-}$ in PS I with 2-methyl-, 2-ethyl-, and 2-ethyl-α,α-d_2-1,4-naphthoquinone in the A_1 binding site. The characteristic hfs 1:3:3:1 for $-CH_3$ group and 1:2.1 for $-CH_2-$ group are indicated.

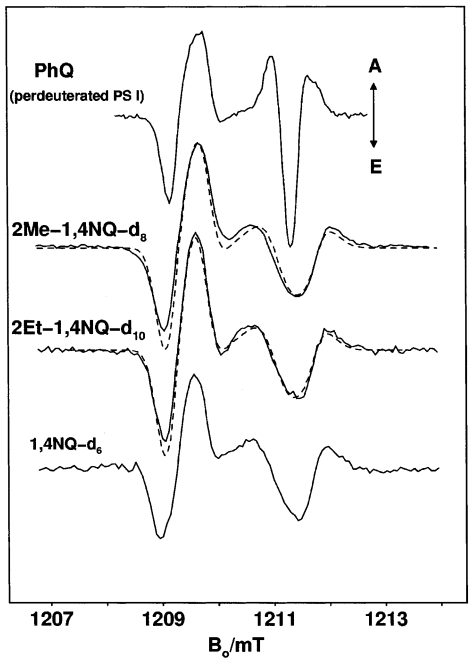

Figure 5. Q-band, 80 K spin polarized transient EPR spectra of $P_{700}^{+}NQ^{-}$ in PS I. Comparison from top to bottom of deuterated PS I, deuterated 2-methyl- and 2-ethyl-1,4-naphthoquinones, and deuterated 1,4-naphthoquinone in the A_1 binding site. Broken lines are simulated spectra; for simulation parameters, see Table 1.

low spin density because it is ortho to the H-bonded oxygen, whereas the methyl group in PhQ and the ring proton in 2-phytyl-1,4-NQ of the *men*G mutant are meta to the H-bonded oxygen. In contrast, for ethyl- and butyl-1,4-NQ and longer *n*-alkyl-1,4-NQ (not shown), the situation is obviously reversed with the alkyl tail now meta to the H-bonded oxygen and the ring proton in the ortho position.

Orientation of Alkyl NQs in A_1 Site. The unexpected tail position could be related to a different orientation of the quinone headgroup in the protein. The spin polarization pattern of the $P_{700}^{+}NQ^{-}$ state is known to be particularly sensitive to the relative orientation of the *g* tensors $\mathbf{g}(P_{700}^{+})$ and $\mathbf{g}(NQ^{-})$ with respect to the vector $\mathbf{z}_D$ connecting the spin density centers of the respective radical ions.[5] To evaluate the relative orientation of the *g* tensors, the spectral components corresponding to the principal *g* values must be well-resolved; that is, high field/frequency EPR spectra are required. For samples containing deuterated quinones, the Q-band (35 GHz) spectra shown in Figure 5 are sufficiently well-resolved to allow the quinone orientation to be determined. The features on the low-field side of the spectra are known to be due to only the quinone, whereas the spectral contributions on the high-field side are mainly determined by P_{700}^{+}. Correspondingly, the upfield A/E/A feature is narrowed only in the top spectrum of Figure 5, when the chlorophylls of P_{700} are also deuterated along with the rest of the reaction center. For the other spectra, only the NQ cofactor is fully deuterated. Figure 5 includes simulations (broken lines) of the spectra of PS I containing perdeuterated 2-ethyl- and 2-methyl-1,4-NQ using the same orientation of the quinone ring plane as known for phylloquinone in native PS I. The simulation parameters are collected in Table 1. The good agreement between the experimental and simulated spectral patterns suggests that both non-native quinones bind with the same headgroup orientation. Moreover, we have also shown previously that the distance between P_{700}^{+} and Q^{-} is the same as that in native PS I for a variety of non-native quinones.[16] However, as discussed in refs 13, 14, and 17, the octant in which the angles describing the orientation of the quinone lie cannot be determined from the *g* tensor alone. With the PQ vector oriented along the *x* axis of the quinone *g* tensor (see Table 1), four possible orientations for the quinone headgroup are possible. The relative orientation of the hfs tensor as well as the hyperfine couplings, which show that the alkyl tail is meta to the H-bonded oxygen, allow the number of possible orientations to be reduced to two. One of the remaining orientations places the side chains of the 2-alkyl-1,4-NQ where the second aromatic ring of phylloquinone is usually located. Such an arrangement is very unlikely because it would lead to steric crowding and would weaken the $\pi-\pi$ interaction between the quinone and the neighboring tryptophan. Therefore, we conclude from the EPR data that the alkyl chains are attached to the ring position normally occupied by the methyl group.

The bottom spectrum in Figure 5 shows 1,4-NQ-d_6 reconstituted into PS I. The E/A/A/E/A polarization pattern with slightly broadened low field features is significantly different from that reported previously.[18] In the earlier study, the polarization pattern for 1,4-NQ-d_6 was A/E/A/A/E/E compared to E/A/A/E/A for PhQ in PS I. The change in the polarization pattern was best explained by a change in orientation from $\mathbf{z}_D \| x$(PhQ) to nearly $\mathbf{z}_D \| y$(1,4-NQ), whereas the orientation of the *z* axis remained unchanged. The different polarization patterns from different preparations show that the orientation of NQ in PS I apparently depends on the sample preparation procedure. A systematic study of the extraction conditions revealed that successful extraction of the quinone depends crucially on the purity of the hexane used. Because the orientation reported in ref 18 ($\mathbf{z}_D \| y$(1,4-NQ)) is incompatible with an H bond to Leu A722 (B706), it is likely that the loop region containing the leucine may be affected by the presence or absence of an impurity in the hexane. The broadened spectrum for 1,4-NQ in Figure 5 is consistent with a distribution of orientations of the substituted 1,4-NQ molecule perhaps because of a distribution of somewhat different binding site conformations. Such a distribution may also be a consequence

TABLE 1: *g* Tensor and Geometrical Parameters Obtained from Simulations of the transient EPR spectra of $P_{700}^{+}NQ^{-}$[a]

	g_{xx}	g_{yy}	g_{zz}	$\Delta B(Q^{\bullet-})$ mT	α_p	β_p	γ_p	θ_D	φ_D
PhQ-d_{46}	2.0062	2.0051	2.0022	0.25	81.0	126.0	182.0	90.0	0
2- methyl-1,4-NQ	2.0063	2.0051	2.0024	0.34	81.0	126.0	182.0	90.0	0
2- ethyl-1,4-NQ	2.0063	2.0052	2.0022	0.31	81.0	126.0	182.0	90.0	0
2-ethyl-α,α-d_2−1,4NQ	2.0063	2.0052	2.0022	0.36	81.0	126.0	182.0	90.0	0
2-ethyl-1,4-NQ-d_{10}	2.0063	2.0052	2.0022	0.34	81.0	126.0	182.0	90.0	0

[a] PhQ-d_{46} is the perdeuterated phylloquinone in perdeuterated PS I complexes. ΔB is the peak to peak line width in first derivative spectra. $\Delta B(P_{700}^{+}) = 0.31$ mT. The Euler angles α_p, β_p, and γ_p describe the relative orientation of $\mathbf{g}(P_{700}^{\bullet+})$ and $\mathbf{g}(Q^{\bullet-})$.[14] The polar and azimuthal angles θ_D and φ_D describe the orientation of $\mathbf{z}_D$ relative to $\mathbf{g}(Q^{\bullet-})$.

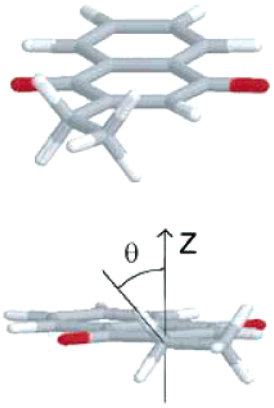

Figure 6. Conformation of the ethyl substituent in the 2-ethyl-1,4-naphthoquinone molecule in the A_1 site PS I as obtained from the analysis of the hyperfine structure. *z* denotes the out-of-plane axis and is equivalent to the p_z orbital axis of the carbon ring atom. $\theta = 30°$ is the dihedral angel between the plane of the C−C and C−H bonds in ethyl group and the axis of the p_z orbital.

of the fact that the 1,4-NQ molecule is the smallest and the only one studied here that does not have an asymmetric substituent. The degree of hydrogen bonding of 1,4-NQ is also reflected in its *g* tensor. The principal values of the g-tensor of A_1^- are known to depend on the presence and strength of H-bonds[14] and in general, the g-tensor anisotropy of semiquinone and related radicals decreases with formation of hydrogen bonds.[19−21] In keeping with the altered orientation, which necessarily breaks the H bond to Leu A722 (B706), the *g*-tensor anisotropy for 1,4-NQ-d_6 incorporated into PS I reported in ref 11 is larger than that of the native PhQ.[22,23] However, from Figure 5, it is apparent that when 1,4-NQ-d_6 is oriented in the same way as PhQ in the A_1 site its *g*-tensor anisotropy is also very similar suggesting that the H-bond Leu A722 (B706) is intact.

Evaluation of Hyperfine Coupling. The well-resolved 1:2:1 hyperfine pattern (see Figure 3 and 4) indicates strong hyperfine coupling to the methylene protons. The value of the isotropic coupling constant of such β protons (e.g., of an ethyl or butyl substituent) is known to be proportional to the π-spin density at the neighboring ring carbon atom (ρ_c^{π}) and to $\cos^2\theta$:

$$a_{iso}(H_\beta) = \rho_c^{\pi}(B_0 + B_2 \cos^2\theta) \qquad (1)$$

where θ is the dihedral angle between the plane of the C−C and C−H bonds and the axis of the p_z orbital (see Figure 6). Standard values for the constants are $B_0 = 9$ MHz and $B_2 = 122$ MHz.[24] The experimental hyperfine patterns in Figures 3 and 4 show that the two hydrogen atoms of the $-CH_2-$ group are magnetically equivalent within experimental accuracy. To that extent, the dihedral angle θ must be the same for both hydrogens as well. Only two conformations of the $C-CH_2-C$ fragment fulfill this requirement. Either the two C−C bonds are in-plane with respect to the NQ ring and both C−H bonds have $\theta = 30°$ as shown in Figure 6 or the second C−C bond points maximally out-of-plane and both C−H bonds have $\theta = 60°$. The $\cos^2\theta$ factor leads to a methylene proton hfs, which is three times larger in the former case. To calculate the hyperfine couplings for these two possibilities, we need the value of the spin density $\rho_c^{(\pi)}$ on the neighboring ring carbon. If we assume that the substitution of the methyl by an ethyl group does not change the spin density distribution of the NQ molecule, we can use the value of $\rho_c^{(\pi)}$ from the hyperfine coupling of 2-methyl-1,4-NQ in PS I. With this spin density, only the configuration of the methylene protons with $\cos\theta = 30°$ can be reconciled with the data. We obtain $|A_{xx}| = 12.2$ MHz, $|A_{yy}| = 16.8$ MHz, $|A_{zz}| = 12.2$ MHz, and $a_{iso} = 13.7$ MHz from simulation of the 2-ethyl-1,4-NQ spectrum shown in Figure 3b. This corresponds to $\theta = 34°$ and is indistinguishable from $\theta = 30°$ within experimental accuracy. The $\theta = 60°$ conformation cannot be completely excluded, but it would require a spin density on the carbon which is three times higher than the already large value found in native PS I. It is very unlikely that such a high spin density would occur. In summary, the most likely configuration is that the alkyl tail resides in the position normally occupied by the methyl group and is oriented so that the two protons straddle the ring plane.

Comparison with the Asymmetric H Bonding of Q_A in Bacterial Reaction Centers (bRC). Asymmetric alternating spin density distribution over the quinone ring as introduced by predominant H bonding to one of the C═O groups has been studied in considerable detail for the corresponding Q_A site in purple bacterial reaction center (pbRC), as reviewed recently.[25] The asymmetry in the spin density distribution has been confirmed experimentally by selective isotope labeling of several ring positions, in particular both nuclei of the C═O groups. In contrast to A_1 in PS I, the C═O group of Q_A in bRC with the dominant H-bond is meta to the ring position at which the tail is attached. Therefore, this ring position carries an increased spin density, and the hfs coupling of the first methylene protons of the tail is large and can be measured readily by ENDOR spectroscopy. In the case of *Rhodobacter sphaeroides* the axially symmetric hfs tensor has been determined with the principal values: $A_{xx} = 8.3$ MHz, $A_{yy} = 5.1$ MHz, $A_{zz} = 5.1$ MHz.[25] According to the X-ray structure, the dihedral angles between the ring plane and the two C−H bonds are +38° and −82°, corresponding to $\theta = 52°$ and 8° in eq 1. Assuming that the measured hyperfine coupling corresponds to the proton with the smaller value of θ, we can use eq 1 to compare the spin density on the ring carbon ortho to the carbonyl group with the stronger H bond in Q_A^- in bRC and A_1^- in PS I. This comparison yields a value for the spin density in PS I that is about three times larger than in bRC. This is consistent with the respective X-ray structures which show two, but inequivalently strong H bonds for Q_A in bRC but only one H bond for A_1 in PS I.

A potentially interesting aspect is revealed by the simulation results of Table 1. The inhomogeneous line width contribution for A_1 in fully deuterated PS I is substantially smaller than that needed for deuterated NQ derivatives in otherwise protonated PS I despite the fact that the two substituents of PhQ should lead to a somewhat larger line width than for the monosubstituted NQ derivatives. This may be indicative of a substantial hyperfine coupling to the proton in the H bond because this coupling will be reduced in fully deuterated PS I but remains the same when only the quinone is deuterated. For this reason, the samples with fully deuterated quinones with normal hydrogen in the H bond are best candidates for a reliable determination of hfs coupling to the H-bonding proton using the full arsenal of advanced pulsed EPR techniques. In particular, pulsed ENDOR spectroscopy of the radical pair $P_{700}^{+}A_1^{-}$ allows the quinone to be observed in the functional radical pair state rather than as a photoaccumulated radical.

Conclusions

Our previous studies with substitution of 2-methyl-1,4-naphthoquinone in PS I of the *men*B mutant[26] and 2-phytyl-1,4-naphthoquinone after inhibition of the methyltransferase gene *men*G[9] demonstrated that neither the phytyl tail nor the methyl group are necessary for maintaining the native quinone orientation and position in the A_1 site of PS I. No difference in the quinone orientation compared to native PhQ was found. However, one asymmetric substituent (2-methyl or 2-phytyl) appeared to be necessary. In this paper, the question was asked how an alternative chain (like a saturated *n*-alkyl chain in the simplest case) would behave. The transient EPR data for 2-methyl-1,4-naphthoquinone (VK_3) substituted in A_1-free PS I are shown here to be equivalent to those obtained with the same 2-methyl-1,4-naphthoquinone exchanged in vitro for the quinone in the *men*B mutant.[26] In contrast, when 2-ethyl-, 2-butyl-, and (even longer) 2-alkyl-1,4-naphthoquinones are substituted in A_1-free PS I, the A_1 site places the artificial quinone with the substituent not in the position where the phytyl-tail of native PhQ is normally located but rather in the position usually occupied by the methyl group. Initial attempts to model the non-native quinones in the A_1 binding site suggest that with this configuration and with the methylene protons straddling the ring the alkyl tail was also directed toward the space normally occupied by the phytyl tail of PhQ. However, there are no obvious reasons why this could not be achieved equally well with the alkyl-tail in the position normally occupied by the phytyl tail in native PhQ. The double bond in the phytyl tail may play a significant role. This is also indicated by the observation that the VK_2 without a methyl group and with a different tail (without a double bond) behaves like native PhQ in PS I.

The methyl group in PhQ certainly adds a contribution to the binding strength of the naphthoquinone headgroup. However, it remains unclear why this extra binding strength would be needed because there does not appear to be any significant selective pressure from poor physiological performance when the methyl group is absent. Note also, that forward electron transfer from the A_1 site to the first FeS center is slowed without the methyl group compared to wild type.[9] It is slowed even further (beyond the limited detectability range of the TR-EPR method) for all 2-alkyl-1,4-naphthoquinones investigated in this study. Further studies are in progress to rationalize the obtained results as a consequence of special properties of the protein structure in the functional A_1 site vicinity.

Acknowledgment. This work was supported by grants from the Deutsche Forschungsgemeinschaft (SFB 498, TPA3 to D.S. and S.Z.) and the Natural Sciences and Engineering Research Council, The Canada Foundation for Innovation, and The Ontario Innovation Trust (to A.v.d.E.).

References and Notes

(1) Jordan, P.; Fromme, P.; Witt, H. T.; Klukas, O.; Saenger, W.; Krauβ, N. *Nature* **2001**, *411*, 909−917.
(2) Angerhofer, A.; Bittl, R. *Photochem. Photobiol.* **1996**, *63*, 11−38.
(3) Stehlik, D.; Möbius, K. *Annu. Rev. Phys. Chem.* **1997**, *48*, 745−784.
(4) Möbius, K. *Chem. Soc. Rev.* **2000**, *29*, 129−139.
(5) van der Est, A. *Biochim. Biophys. Acta* **2001**, *1507*, 212−225.
(6) Fromme, P.; Jordan, P.; Krauβ, N. *Biochim. Biophys. Acta* **2001**, *1507*, 5−31.
(7) Zybailov, B.; van der Est, A.; Zech, S. G.; Teutloff, C.; Johnson, T. W.; Shen, G.; Bittl, R.; Stehlik, D.; Chitnis, P. R.; Golbeck, J. H. *J. Biol. Chem.* **2000**, *275*, 8531−8539.
(8) Semenov, A. Y.; Vassiliev, I. R.; van der Est, A.; Mamedov, M. D.; Zybailov, B.; Shen, G.; Stehlik, D.; Diner, B. A.; Chitnis, P. R.; Golbeck, J. H. *J. Biol. Chem.* **2000**, *275*, 23429−23438.
(9) Sakuragi, Y.; Zybailov, B.; Shen, G.; Jones, A. D.; Chitnis, P. R.; van der Est, A.; Bittl, R.; Zech, S. G.; Stehlik, D.; Golbeck, J. H.; Bryant, D. A. *Biochemistry* **2002**, *41*, 394−405.
(10) Biggins, J.; Mathis, P. *Biochemistry* **1988**, *27*, 1494−1500.
(11) Sieckmann, I.; van der Est, A.; Bottin, H.; Setif, P.; Stehlik, D. *FEBS Lett.* **1991**, *284*, 98−102.
(12) van der Est, A.; Hager-Braun, C.; Leibl, W.; Hauska, G.; Stehlik, D. *Biochim. Biophys. Acta* **1998**, *1409*, 87−98.
(13) Kamlowski, A.; Zech, S.; Fromme, P.; Bittl, R.; Lubitz, W.; Witt, H. T.; Stehlik, D. *J. Phys. Chem. B* **1998**, *102*, 8266.
(14) Zech, S. G.; Hofbauer, W.; Kamlowski, A.; Fromme, P.; Stehlik, D.; Lubitz, W.; Bittl, R. *J. Phys. Chem.* **2000**, *104*, 9728−9739.
(15) O′ Malley, P. J. *Biochim. Biophys. Acta* **1999**, *1411*, 101−113.
(16) Zech, S. G.; van der Est, A. J.; Bittl, R. *Biochemistry* **1997**, *32*, 9774−9779.
(17) Kandrashkin, Yu.; van der Est, A. *Spectrochim. Acta A* **2001**, *57*, 1697−1709.
(18) van der Est, A.; Sieckmann, I.; Lubitz, W.; Stehlik, D. *Chem Phys.* **1995**, *194*, 349−360.
(19) Kaupp, M.; Remenyi, C.; Vaara, J.; Malkina, O. L.; Malkin, V. G. *J. Am. Chem. Soc.* **2002**, *124*, 2709−2722.
(20) Engstrom, M.; Owenius, R.; Vahtras, O. *Chem. Phys. Lett.* **2001**, *338*, 407−413.
(21) Engstrom, M.; Himo, F.; Graslund, A.; Minaev, B.; Vahtras, O.; Agren, H. *J. Phys. Chem. A* **2000**, *104*, 5149−5153.
(22) van der Est, A.; Prisner, T.; Bittl, R.; Fromme, P.; Lubitz, W.; Möbius, K.; Stehlik, D. *J. Phys. Chem. B* **1997**, *101*, 1437−1443.
(23) MacMillan, F.; Hanley, J.; van der Weerd, L.; Knupling, M.; Un, S.; Rutherford, A. W. *Biochemistry* **1997**, *36*, 9297−9303.
(24) Carrington, A.; McLachlan, A. *Introduction to Magnetic Resonance*; Harper and Row: New York, 1969; Chapter 7.
(25) Lubitz, W.; Feher, G. *Appl. Magn. Reson.* **1999**, *17*, 1−48.
(26) Johnson, W. J.; Zybailov, B.; Jones, A. D.; Bittl, R.; Zech, S. G.; Stehlik, D.; Golbeck, J. H.; Chitnis, P. R. *J. Biol. Chem.* **2001**, *276*, 39512−39521.